

Hinged wingtip modelling in NeoCASS based on Airbus AlbatrossONE

PIR - Projet Innovation Recherche

Francesco Marzagalli*

advisor: Joseph Morlier†

*Student at Isae-Supaero (Institut Supérieur de l'Aéronautique et de l'Espace), Toulouse, France
Email: francesco.marzagalli@student.isae-supero.fr

†Professor at Isae-Supaero (Institut Supérieur de l'Aéronautique et de l'Espace), Toulouse, France
Email: joseph.morlier@isae-supero.fr

25th June 2020

Abstract—This paper deals with the modelling of a new aircraft wing-design with NeoCASS software. Inspired by nature, Airbus has developed a remote-controlled demonstrator called AlbatrossONE, which is characterized by hinged wing tips. The advantage is reducing drag, stress and, at the same time, handling turbulence and gust effect in a more comfortable way. After an introduction on AlbatrossONE project, on the concept of "semi aeroelastic hinge" (SAH) and on the main feature of NeoCASS software, the paper will report the analysis conducted via NeoCASS on a modelled aircraft equipped with folding wing tips. The main results will be analysed and compared with respect to the traditional wing configuration.

I. CONTEXT

Folding wing tips are not a new design concept in aviation. In the past few years combat aircraft have been designed in order to take up little space in aircraft carriers for example. However, nowadays this design feature is getting more and more interesting due to other applications. The latest version Boeing 777 already includes this option in order to limit the space occupied on the ground, in airports. The challenge now is to exploit this design to improve performance and to attain load alleviation, which can be translated or in lighter wings or in larger aspect ratio, in this case reducing the induced aerodynamic drag. As questioned in [1], this device allows the wingtip to rotate and such a mechanism can even be exploited during flights in order to improve performance. However, free wingtips are not flawless: as highlighted in [2] zero stiffness hinges can lead to undesired effects during cruise for example. During leveled flight, aerodynamic performance can be worsened by constant deflection of the wingtip due to static loads

or by oscillating phenomena due to dynamic loads. Here comes the idea of a semi aeroelastic behaviour for this device, implemented with a kind of brake which frees the wingtip in case of need. As the research [1] stated, load alleviation can be attained by letting the wing tip fold and adjusting both the hinge orientation (described by a *flare angle* Λ) and the spring properties (e.g. stiffness). In fact a non-zero hinge angle introduces a local decrease in the angle of attack as the following formula explains:

$$\alpha_{wt} = -\text{atan}(\tan\theta \sin\Lambda) \quad (1)$$

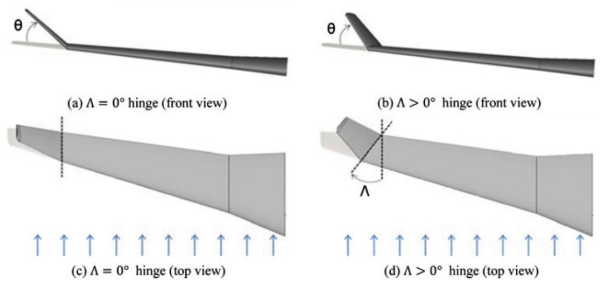


Fig. 1: Hinge line folding wingtip [1]

A series of experiments on numerical modelling have been performed by [1] in order to find an optimum configuration both varying the flare angle ($0^\circ \div 25^\circ$), the weight (100kg or 943kg) and the torsional stiffness of the device, starting from a fixed one up to an almost free one. The model was built so that the wingspan was increased by 25% thanks to the folding device. The main presented results were the following:

- a reduction of 30% in the wing-root loads was obtained in the case of a low stiffness 25° hinge with respect to the fixed one;
- the loads were only 4.36% higher than in the baseline model without folding wing tips;
- flutter analysis shown how a low mass for the device in the case of 25° hinge was beneficial for all stiffness, while for the 0° hinge model flutter speed was very high for all the values of mass and stiffness;
- the gust response proved load reductions for high swept hinge angles, low wingtip mass and stiffness.

Furthermore, in the simulation of a semi aeroelastic wingtip [2] it was proved that the system response to a discrete gust was positive: the behaviour was statically stable with a max fold angle of 25° and dynamically stable thanks to an aerodynamic damping contribution from the flapping motion. As the bending moment across the hinge drops to zero, bending moments at the wingroot were decreased.

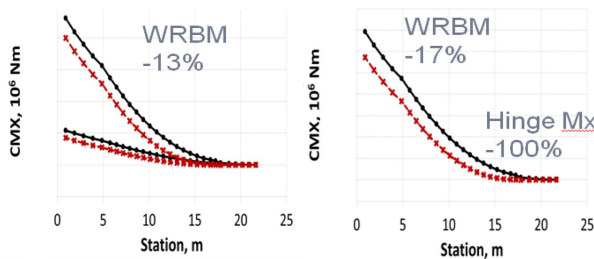


Fig. 2: Wing-root bending moment for up/down gust (right) and 2.5g maneuver (left), red for free hinge and black for fixed hinge [2]

The same research [2] simulated studies on an aircraft loosely based on A320 family, extending the span from 36m to 45m with the aim of studying loads and flutter both for a fixed and a free hinged wingtip. Again, as shown in figure (2), the results were in favour of the free hinge, in the gust case wing-root bending moment was reduced by 13% while in a 2.5g maneuver by 17%. However flutter speed showed to be higher with the fixed hinge, as already had been found by [1]. In a second model a heavier (2.5 times) wingtip was considered, again the free wingtip was characterized by a strong flutter coupling due to the the flapping mode coupling with the first wing bending mode. This is a dangerous risk that can be avoided by adding mass to the wing tip and by tuning the flare angle to 15° (instead of 25°).

hence it was proved that free hinge could induce flutter, but that it could be stabilised by careful shrewdness.

Later studies [3] dealt with aeroelastic flight dynamics coupling due to the installation of a semi aeroelastic hinge and proved that the baseline model had the same handling qualities and dynamics response as the free-hinge one.

Further simulations [4], [5] tried to find a solution to the oscillating deflections of the wingtip which spoils cruise aerodynamic performance. The concept of a non linear hinge spring was introduced in order to enable the folding mechanism when aerodynamics loads were greater than a threshold value. In this simulation a 100Kg wingtip model with a 25° hinge and a spring stiffness of 1Nm/rad were considered. When the loads generated a wing moment greater than a defined value M_{max} the wingtip was allowed to fold, such an idea was realised by applying on the hinge restoring moments ($M_{NL} = -K_\theta\theta$) through a piecewise linear spring whose stiffness varied as follows:

$$\begin{cases} K_\theta = 1.E12 \text{Nm/rad if } K_\theta\theta \leq M_{max} \\ K_\theta = 1.E0 \text{Nm/rad if } K_\theta\theta > M_{max} \end{cases} \quad (2)$$

Even a hinge moment provided by a linear damping element was considered:

$$M_{damp} = -D_\theta \dot{\theta} \quad (3)$$

The gust response was analysed at 25.000ft at $M=0.6$, different gust length and speed were considered along with different values for hinge damping factor and threshold value. The results highlighted that a good load alleviation was obtained when both the threshold and damping values were low, as the wingtip was allowed to fold soon and quickly. Higher values showed a delayed and less effective response, due the less time available to counteract the perturbation. Even the damping factor proved itself to be positive, it reduced the inertial loads of the wingtip, but a good compromise was sought in order not to decrease the load relief ability (related to a fast response). The investigation on gust response was analysed again in [5] where the wingtip was released as an increment of 1° in the angle of attack was detected. The semi aeroelastic wingtip was the most effective compared to the fixed and a free ones, reducing gust peak and 1g loads, as shown in figure (3).

Related work to load alleviation was presented by [6] and [7]. In this case main attention was concentrated on the concept of an active wingtip extension, hence giving a new insight into this topic. The device was designed such to have a trailing edge control surface, with an



Fig. 3: Wing-root bending moment for release and gust excitation (red = free hinge, blue = fixed hinge, black = SAH) [5]

extension set by running an optimisation problem. Even if this simulation gave a different nuance to the problems submitted before, the results were again satisfying, the active control on the surface proved to lead load reduction both in gust and maneuver cases. Besides much theoretical work, even a concrete application of it must be taken into consideration.

Presented in June 2019, the Airbus AlbatrossONE [8] embodies the innovative idea of the semi aeroelastic hinge wingtip. This small scale remote-controlled aircraft is based on the A321 and has already been tested in flight in Filton (UK) both in the fixed and free hinge configuration. The demonstrator is not dynamically scaled, the purpose of the project is just to provide a qualitative but concrete application of the SAH device in order to test previous theoretical work [1], [2], [4], [5]. Besides, another objective of the demonstrator is proving that the wing aspect ratio of an Airbus-like aircraft can be approximately doubled without any worsening on loads and handling qualities. Different wingspan for the demonstrator have been conceived:

- A 2.6m wing span with no wing tips, equivalent to a 35m wing span;
- A 3.2m wing span equivalent to a 45m wing span, one with fixed wing tips, and one with the wing tips free to rotate about their hinges;
- A 3.7m wing span equivalent to a 52m wing span, one with fixed wing tips, and one with the wing tips free to rotate about their hinges.

The main technical characteristics of AlbatrossONE, as reported by [9], are the wings made in carbon fibre reinforced plastic, the fuselage in fiber glass supported by plywood frames, electric fan motors and a cruise speed of 25m/s. Again, the demonstrator does not repro-

duce real aircraft behavior, but it has been considered representative in a qualitative sense. Flight test results were satisfactory, the wingtips were stable, the pilots had no problem in handling the aircraft with free wingtips and bending moments measured in different parts on the wingspan showed a decreasing trend for free hinge case [9], thus providing load alleviation.

II. PROBLEM STATEMENT

The purpose of this paper is to present a model inspired by the AlbatrossONE and to reproduce qualitatively its performance via NeoCASS (Next generation Conceptual Aero Structural Sizing) a suite of Matlab modules that merges state of the art computational, analytical and semi-empirical methods to deal with all the aspects of the aero-structural analysis of a design layout at conceptual design stage [10]. As presented in [11]–[13] NeoCASS is made up of different modules:

- WB (weight and balance), which estimates masses and their location;
- GUESS (Generic Unknowns Estimator in Structural Sizing), which gives an analytical sizing of the airframe, generates both a structural stick model (by means of semi-monocoque method) and a FE mesh;
- SMARTCAD (Simplified Models for Aeroelasticity in Conceptual Aircraft Design), which solves different aero-structural problems (trimmed solution, modal analysis, flutter computation, steady and unsteady aerodynamic analysis and static aeroelastic analysis), exploiting both a beam model and Vortex/Doublet Lattice Method.
- MDO, which ameliorates initial sizing and meets aeroelastic constraints

The geometric representation of the aircraft is stored in a *.xml* file and the geometry database is developed in an ad-hoc module called ACbuilder, a graphic environment where the user can interact with the model.

Aware of the potential of NeoCASS, it is possible to imagine how to model a folding wingtip in order to analyse the advantages of such a configuration and to reproduce the results reported by AlbatrossONE.

III. BUILDING THE BASELINE MODEL

The first step to take was modeling an Airbus A321 in NeoCASS in order to exploit it as reference. Different sources have been taken into consideration to fulfill this purpose, as reported in [14]–[17]. Unfortunately the reproduction of the aircraft was affected by some drawbacks, some data were unavailable due to the fact

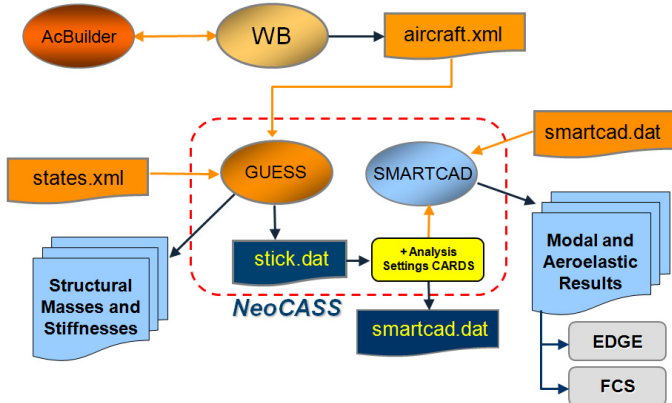


Fig. 4: NeoCASS layout

that they are very sensitive and so the companies prefer not to make them public. The kind of airfoil used in the wings, for example, is something very particular for each aircraft and thus not much information is given on that. Therefore in this case standard characteristics were chosen to represent the aircraft, for example for the airfoil a NACA 0012 was used, which is the standard one given in NeoCASS. Also speaking of materials it should be recognised that the features of standard aluminium alloy was considered.

As shown in figure 4 first of all a *.xml* file, which is built by ACbuilder, is needed to start the analysis on the aircraft. In ACbuilder module the shaping of the aircraft starts with the definition of the geometry of the fuselage, the main data are collected in the following table (I):

Fuselage Geometry	
Fuselage length	44.51m
Vertical diameter	4.14m
Horizontal diameter	3.95m

TABLE I

Other parameters of less importance were used to shape the fuselage in a more realistic way either for the nose or for the tail. The next components to take into consideration were the lifting surface. The wing main properties are reported in table (II) as well as those of the tailplane.

Once this was completed in ACbuilder the geometry of the aircraft had been defined, the next steps were addressed to define the fuel properties and the mass onboard the aircraft. Conventional configuration have been considered in order to match as well as possible the real features of the A321. Anyway these data are used in a second instance by the GUESS module as a starting point

Wing Geometry	
Wing area	122.4m
Wing span	34.1m
Aspect ratio	9.5
Spanwise Kink 1 & 2	0.37 & 0.7
Taper kink 1 & 2	0.589 & 0.37
Taper tip	0.19
Leading edge sweep	25°
Dihedral angle	6°
Airfoil	NACA 0012

Tailplane geometry	
HT area	27m
HT span	12.45m
VT area	21.5m
VT span	6.26m
HT sweep angle	25°
VT sweep angle	34°
Airfoil	NACA 0012

TABLE II

to complete the aircraft sizing, as it is shown afterwards. Once this part is completed a model of the aircraft can be visualized (Fig.5):

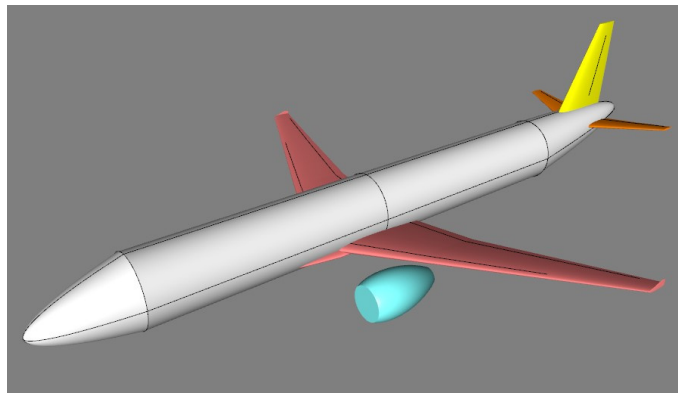


Fig. 5: 3D view of the model after geometry definition

Finally the technology section must be considered: here the number of nodes of the beam model structure, the number of panels for the aerodynamic mesh and spars location have been defined. Furthermore here the material properties can be defined and as already mentioned standard aluminium alloy was considered. This section let the user interact both the geometry of the beam model and the aerodynamic mesh, as figure (6) shows. Once the model was ready the Weight and Balance module provided a first estimate of mass and masses distribution that was later refined by the GUESS module. The WB module took into consideration all the aircraft components previously defined in order to calculate ei-

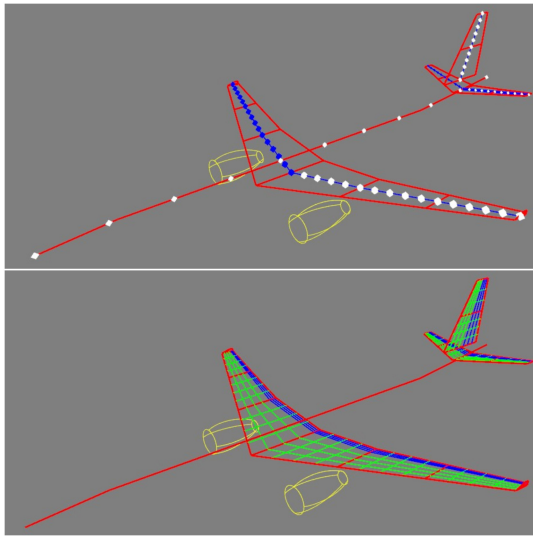


Fig. 6: Beam model and aerodynamic mesh

ther their weight and location with respect to a reference frame which has its origin in the aircraft nose. By considering the aircraft a solid with constant density a starting inertia matrix was also calculated. When the *.xml* file was ready all the data have been passed to NeoCASS main routine to continue the modelling.

GUESS module was then invoked in order to refine the previous weight prediction and to estimate stiffness and load-bearing material distribution. To this end, sizing maneuvers have been defined by exploiting the *EASA automatic selection* for cruise, pull-up and other maneuvers at different load condition. The starting data considered were the following:

EASA automatic selection	
Cruise speed (V_c)	$231.4m/s$
Maximum Mach number (MD)	0.89
Max ceiling altitude (HMAX)	$11900m$
Clean mac lifting coefficient	1.4
Reference surface	$122.4m^2$
Landing gear efficiency	0.8

TABLE III: Sizing maneuvers input

The sizing maneuvers are stored in a *.inc* file which is used by GUESS module to run the final sizing of the aircraft. Thanks to the Vortex Lattice Method (VLM) aerodynamics and inertial loads were calculated by trimming the aircraft. GUESS determines the minimum structural mass that avoids structural failures in the most critical conditions by considering total shear force and bending moment along the fuselage and wings. After

running GUESS module different data were obtained both for weight, mass distribution, components center of gravity and aircraft balance. All the results are reported in a *.txt* file, in the table (IV) those of major importance are summarized.

Aircraft Weights	
Operative Empty Weight (OEW)	$34520.91kg$
Max Zero Fuel Weight (MZFW)	$54478.71kg$
Maximum Take Off Weight (MTOW)	$76778.71kg$

TABLE IV: Main GUESS results for baseline aircraft weights

At this point some consideration can be made, since the Maximum Take Off Weight for an Airbus A321 is about 80 tons (different weights are due to the variants of the model) the model built in NeoCASS seems to be sufficiently representative of the original Aircraft; this is an important starting point for an overall satisfying analysis. Anyway inaccuracies are always present either because the model within the geometry input file is simplistic (e.g it doesn't describe accurately fuselage and lifting surfaces) and due to the fact that load computation is also affected by this lack of precision. Another interesting output of this section is the aeroelastic model described in figure (7) where both the aerodynamic mesh and the stick beam model are represented.

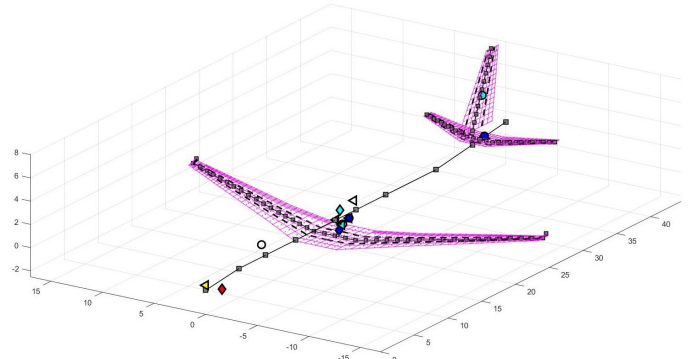


Fig. 7: Aeroelastic model

Once the stick beam model with lumped masses was ready, the SMARTCAD module has been invoked to continue the modeling process considering the static, dynamic and aeroelastic behaviour of the airframe. For each analysis different cards were written as ASCII files derived from NASTRAN formats, a well-known standard in aerospace. Two analyses in particular have been considered: static trim aeroelastic analysis, and gust response.

IV. ANALYSIS DESCRIPTION

When a trim aeroelastic analysis is desired a dedicated *.dat* file must be built. In this file different types of information are stored and other input files are recalled. Using NASTRAN format, the file containing the information about mass distribution and the stick beam model which come from the GUESS module must be included. Another file to be included is the one which contains the flight condition and maneuvers whose analysis is desired. For this study table (VI) collects the maneuvers that were considered. Finally, some other parameters must be defined, such as the reference chord, the reference surface and the wingspan.

Reference Chord	Wingspan	Reference surface
3.59m	34.1m	122.4m ²

TABLE V: Reference parameters for trim analysis

Once the input file is ready the aeroelastic analysis can be performed. The solver is based in the Vortex Lattice Method (VLM), in which *Prandtl-Glauert* correction is used to take into consideration comprehensibility effects.

Cruise	
Mach	0.78
Altitude	11000m
Pull-up	
Mach	0.25
Vertical acceleration	2g
Sideslip levelled flight	
Mach	0.3
Sideslip angle	6°

TABLE VI: Flight condition analysed in aeroelastic trim

After the analysis all the results for the considered flight condition are stored in a *.txt* output file and the struct type variable *beam.model* contains all the data that can be post-processed. As it will be shown afterwards most focus will be given on out of plane bending moment.

For the aeroelastic dynamic response, on which the solution for the gust response is based, the analysis is more demanding both for theoretical knowledge and for numerical simulation. The dedicated module in NeoCASS for dynamic analysis is called NeoRESP. As for the trim analysis, a dedicated input *.dat* file is required, in which the the aircraft models must be included both for mass and stick beam configurations. Following NASTRAN format all the flight reference conditions must be

defined in terms of flight speed V_∞ (TAS), air density ρ and flight Mach number M_∞ . These parameters have been chosen with respect to the cruise flight condition, as follows:

Flight speed V_∞	Air density ρ_∞	Mach number M_∞
231m/s	0.32kg/m ³	0.78

TABLE VII: Reference parameters for dynamic analysis

This parameters are required to solve the aeroelastic response, presented in equation (4).

$$-\omega^2 M + i\omega C + K - q_\infty H_{mm}(k, M)q(\omega) = \\ -q_\infty H_{mg}(k, M)V_g(\omega) \quad (4)$$

The required parameters are in fact used to define the dynamic pressure q_∞ through ρ and V_∞ , the reduced frequency k of the problem, through reference chord and the matrices H_{mm} and H_{mg} , through M_∞ . Then some information on modal analysis is required: for example the maximum frequency to analyse and the all the different reduced frequency for the dynamic analysis. Furthermore the number of modes to follow, which defines the modal basis, has been fixed at 20. Before the definition of the gust shape some other reference parameters must be included for the Double lattice solver, which is *SOL 146* for NASTRAN standard, as table (VIII) shows:

SREF	MXS	CHD	RHO	NS	BREF
122.4m ²	350m/s	3.59m	0.32kg/m ³	50	34.1m

TABLE VIII: Reference parameters for DLM

where,

- SREF is the reference surface;
- MXS is the max speed in flutter tracking;
- CHD is the reference chord;
- RHO is the air density;
- NS is the number of velocity steps in flutter tracking [0;MXS] range
- BREF is the wingspan.

Finally, The gust settings must be defined. The spanwise gust profile has been considered uniform and gust velocity (V_g) was considered only in the direction of vertical z-axis. Due to the vertical gust the aircraft experiences increased loads as the angle of attack is larger than the trim condition.

$$\Delta\alpha_g = \tan^{-1} \left(\frac{V_g}{V_\infty} \right) \approx \frac{V_g}{V_\infty} \quad (5)$$

As the normative requires, a *1-cos* gust has been taken into consideration in order to model the time evolution of the vertical gust velocity which hits the aircraft:

$$TFUN = \frac{1}{2}[1 - \cos(\omega t)] \quad (6)$$

As the maximum amplitude is unitary, a second parameter must be considered in order to model the maximum vertical speed of the gust, this parameter is called *MAG* (maximum amplitude gust) and it represents the gust scale factor. Therefore the vertical speed of the gust is defined as:

$$V_g = MAG \cdot TFUN \quad (7)$$

The gust CARD follows NASTRAN format and it is composed by different fields which collect the parameters used to build the gust profile. The choices for this analysis are reported in table (IX).

MAG	Duration	ΔT	Delay	TFUN
15m/s	0.5s		0s	$\frac{1}{2}(1 - \cos(\frac{2\pi}{0.5}t))$

TABLE IX: Reference parameters for gust profile

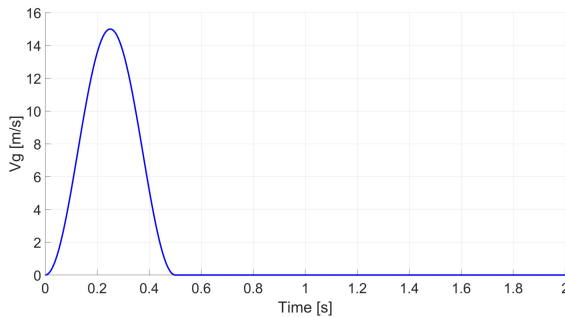


Fig. 8: Gust profile evolution in time

In this way the pulsation of the cosine function is rebuilt considering the duration of the gust event, so that $\omega = \frac{2\pi}{\Delta T}$. The gust profile for all gust analysis is represented in figure (8). Once the gust definition was completed the dynamic analysis was launched. The post-processing was mainly focused on the vertical displacement of the aircraft and on the evolution in time of the increment wing-root bending moment due to the gust excitation. These results are presented in a dedicated section.

V. HINGE DEVICE MODELLING

First of all a second aircraft model was realised in ACbuilder environment. The new aircraft has the same characteristics as the A321 but the wingspan was increased up to 45m in order to reproduce the work done on Airbus AlbatrossONE. For the same reason the second *spanwise kink* was placed at 75% of the wingspan. This choice has been made in order to reproduce the wingtip hinge position in AlbatrossOne, with this *kink* declaration in fact the solver places in this position a structural node, whose interest is shown afterwards. This new model has the interesting feature that the wing aspect ratio is now grater than the baseline one, 16.54 vs 9.5. The main gain of this is a reduction in the induced drag coefficient C_{d_i} , as the following equation (8) shows:

$$C_{d_i} = \frac{(C_l)^2}{\pi \cdot AR \cdot e} \quad (8)$$

where,

- C_l is the lift coefficient;
- e is the *Oswald efficiency* which accounts for the lift distribution on the wing;
- AR is the wing aspect ratio.

However the wider wing version has a main setback which is represented by structural problems as bigger lever arms increase the bending moment especially at the wing-root. The aim of introducing the hinge device was just to find a solution for load alleviation.

The idea to mimic the behaviour of an hinge device laid on the definition of a NASTRAN element which is called CELAS. As reported in [18], this element defines a scalar spring element which has been exploited to reproduce the degree of freedom given to the wingtip through the hinge device. First of all, as previously done with the baseline model, the GUESS module was executed considering the same sizing maneuvers as the baseline model in order to obtain weight distribution, aircraft balance and the stick beam model. As can be deduced by comparing table (X) and (IV) the wider wingspan involves a weight increase of about 3 tons.

Aircraft Weights	
Operative Empty Weight (OEW)	37541.78kg
Max Zero Fuel Weight (MZF)W	57499.58kg
Maximum Take Off Weight (MTOW)	80099.58kg

TABLE X: Main GUESS results for aircraft weights

Since the file with the structural model was accessible, it was properly modified to reproduce the desired behaviour of the wingtip. The whole process is described

for the right wing, as an analogous one was proposed for the left wing. Among the GUESS output there is a .inc file in NASTRAN format where information about the material, the nodes, the beam, the aeronodes, lifting surface, structural interpolation set and lumped masses definition or properties. The idea was to take in consideration the node were the hinge was designed to be placed and make a copy of it. Therefore from node 2014 a copy was made and called 8001 with the same spatial coordinates referred to the basic frame. For the meaning of each entry the reference is [18].

Nodes definition							
GRID	2014	0	24.44	16.96	0.268	0	0
GRID	8001	0	24.44	16.96	0.268	0	0

Once the set of structural nodes was modified the beam definition was taken into consideration. The node 2014 was shared between the beam 2013 and 2014, the first bar definition was left unmodified, while the first node of the second bar was replaced: instead of node 2014, node 8001, the node copy introduced before, was placed as the first node of bar 2014. In order to restore the connection between bar 2013 and 2014 which were at this point disconnected, an elastic CELAS element was exploited as anticipated at the beginning of this section (V). Actually, six CELAS elements where introduced between the nodes 2014 and 8001 of the bars 2013 and 2014, each one for one degree of freedom.

Beam definition							
CBAR	2013	2013	2013	2014
CELAS	8001	A	2014	1	8001	1	
CELAS	8002	B	2014	2	8001	2	
CELAS	8003	C	2014	3	8001	3	
CELAS	8004	D	2014	4	8001	4	
CELAS	8005	E	2014	5	8001	5	
CELAS	8006	F	2014	6	8001	6	
CBAR	2014	2014	8001	2015

It is important to underline the meaning of the third entry for CELAS elements: it is the stiffness of the spring which must be chosen carefully. The stiffnesses A, B, C, E, F, G were set with a very high value ($\approx 1e+15 \text{ Nm/rad}$ or N/m) because the related degrees of freedom had to be locked, as the two nodes connected are in reality the same node. D stiffness was instead set with different values in order to see the hinged wingtip effect on the aircraft from low values (not too much because of numerical problems) to higher ones. In fact the fourth entry for the CELAS element models a rotational

stiffness which enables the wing tip to fold about the global x-axis (aligned with the fuselage axis). Finally, the definition of the interpolation node set between the beam model and the aerodynamic mesh was modified to properly transfer the loads through the splines after the node splitting. In particular the set definition before the node 2014 was left unmodified, as its behaviour was unchanged, while the portion after this node (which is the one free to fold thanks to the hinge) was altered using as the first node not the 2014 but the 8001. As shown in figure (9), which represents the trim solution for cruise, the model for the hinge mechanism works as the wing tips are free to fold independently from the remaining part of the wing.

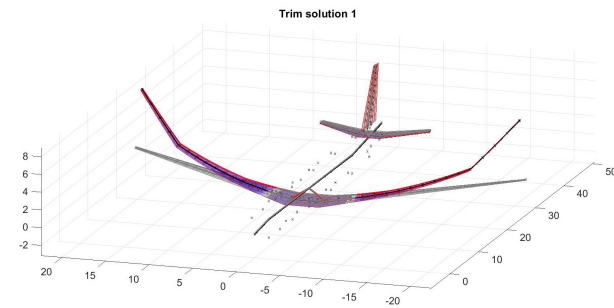


Fig. 9: Hinged wingtips AC, trim solution for cruise

In order to study the effect of different hinge position and rotational stiffnesses, different configurations have been taken into consideration. In particular 5 hinge positions, between 75% and 93% of the wingspan, and 4 values for the hinge stiffness were proposed, as reported in table (XI), for a total of 20 different configurations.

Hinge Position				
75%	81%	84%	88%	93%
Rotational Stiffness				
$1e + 03$	$1e + 04$	$1e + 05$	$1e + 06$	Nm/rad

TABLE XI: Different hinge positions and stiffnesses configurations considered

VI. RESULTS

The following section takes into consideration the main results of this research. As mentioned before, main focus is given on the evolution of the wingspan bending moment in case of cruise and 2g pull-up manoeuvre for the trim analysis. Wing-root bending moment (WRBM)

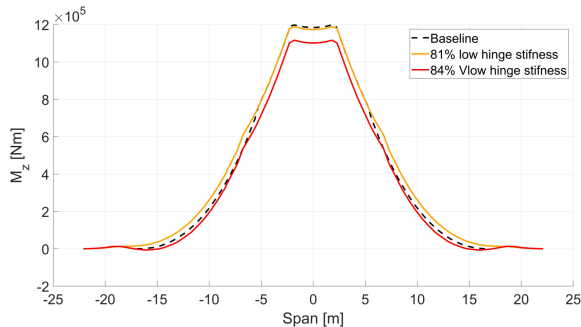


Fig. 10: Wingspan bending moment in Cruise - Best results and comparison

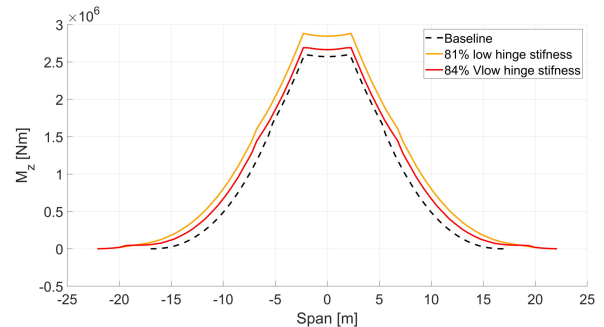


Fig. 12: Wingspan bending moment in 2g pull-up - Best results and comparison

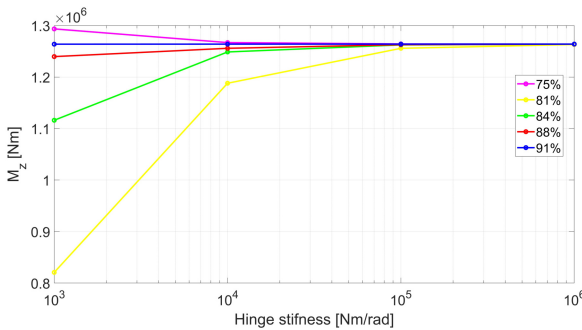


Fig. 11: Hinge stiffness and position effects on Wing-root bending moment - Cruise

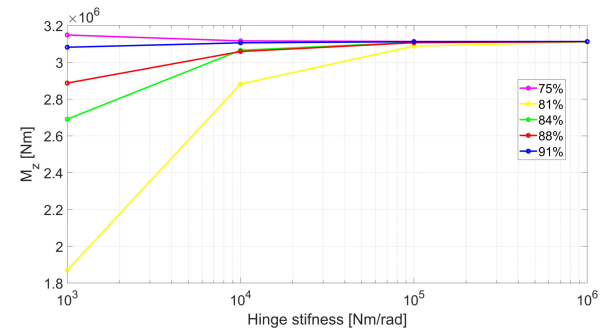


Fig. 13: Hinge stiffness and position effects on Wing-root bending moment - Pull-up

and centre of gravity (CG) vertical displacement evolution in time are instead the main outputs for the gust dynamic analysis. For the sake of clarity just the best configurations are reported and properly commented.

A. Trim Analysis

Figure (10) shows the two best configurations in case of cruise with respect to the baseline model where neither wingspan increase nor hinge device are implemented. The best results are related to very low or low hinge stiffness, which was expected due to previous research work. However, the hinge configuration at 75% of the wingspan with a very low stiffness (red one in figure) shows an unexpected behaviour, the wing-root bending moment is reduced by 7% with respect to the baseline, which is over optimistic in relation to previous theoretical studies. The other configuration (orange one) induces a load alleviation of 1% in the WRBM: this result is much more realistic and conclusive as the hinged wingtip aircraft has a higher aspect ratio wing than the baseline model.

The same considerations can be made for the 2g Pull-up manoeuvre. The best results are again related to a low hinge stiffness, as expected, placed about the 80% of the

wingspan. In this case the loads are much higher than in the cruise flight, as figure (12) points out. In this case no load alleviation is obtained because respectively the maximum load is 3.8% and 11% higher than the baseline case. However it can be stated that the best results are qualitatively correlated to low hinge stiffnesses. In this regard, figures (11) and (13) are remarkable: in both cases a clear correlation between the hinge stiffness and position is showed with the maximum bending moment. Except for one case, the one with the hinge placed at 75%, the qualitative trend predicts a higher WRBM for a higher stiffness, as desired.

B. Gust Analysis

Even though every hinged wingtip leads to benefits in terms of CG maximum vertical displacement, figure (14) shows that the best configuration is related to high hinge rotational stiffness, with a 25% decrease in vertical displacement with respect to the baseline model. Besides, in figure (15), is reported the maximum vertical displacement trend with the effect of hinge position and stiffness: a clear correlation between the parameters is noticeable, even if in this case the trend in opposition with the load alleviation case. As anticipated, higher stiffnesses

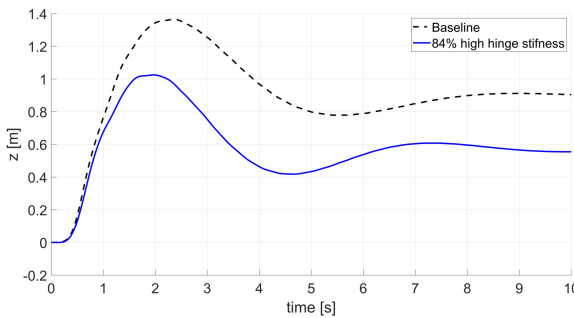


Fig. 14: CG vertical displacement - Best results and comparison

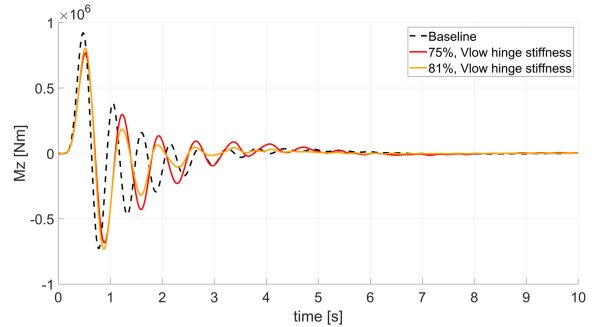


Fig. 16: Wing-root bending moment - Best results and comparison

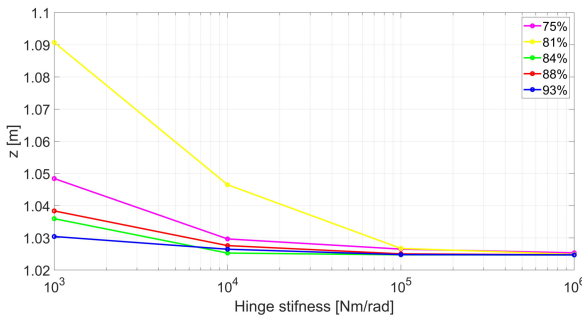


Fig. 15: Hinge stiffness and position effects on CG vertical displacement

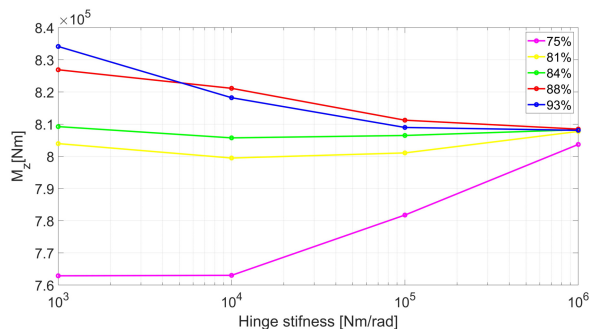


Fig. 17: Hinge stiffness and position effects on wing-root bending moment

result in lower vertical displacement, but anyway the differences are very subtle.

Concerning the wing-root bending moment's evolution in time, the hinge device proved to be beneficial for load alleviation in each of the 20 configurations analyzed, but figure (16) illustrates the two best hinge configurations. In both cases low hinge stiffness proves to be the best choice, as expected by previous work, but if the hinge is placed at 75% the peak reduction is higher than in the 81% configuration: -17% vs -13%. Nevertheless the first configuration has a much slower dynamic response than the second one, whose oscillations are more damped. As often happens in engineering studies, the best result is the compromise between different aspects that should be taken into account. However, in this case no clear correlation has been found between maximum WRBM and the considered parameters, hinge position and stiffness. In figure (17) no clear relation is represented between the parameters of interest, and so here further and deeper work is required.

VII. CONCLUSION AND FUTURE WORK

This paper has presented a proposal to model and reproduce the performance of hinged wingtips on a

conventional aircraft using NeoCASS. The purpose of this research project has been achieved in a sufficiently satisfactory way: after a deep explanation of how the models to be analysed have been built within NeoCASS interface, an idea of how to mimic the folding mechanism was proposed and proved to reproduce the desired behaviour. As expected, generally the best results have been attained with low hinge rotational stiffness placed about at the 80% of the wingspan. However some deeper analysis is required, for example in order to model the flare angle, which was highlighted in the bibliography as of key importance to improve performances, and to ameliorate the correlation between the considered parameters in the gust analysis case.

VIII. ACKNOWLEDGMENTS

Finally, I want to thank Dr. J.Morlier, ISAE-SUPAERO professor, for both the care and the time he dedicated to me during these months, as well as F.Toffol, Politecnico di Milano PhD, who helped me in the understanding of NeoCASS logic and main functionalities.

REFERENCES

- [1] A. Castrichini, V. Hodigere Siddaramaiah, D.E. Calderon, J.E. Cooper, T. Wilson, and Y. Lemmens. Preliminary investigation of use of flexible folding wing tips for static and dynamic load alleviation. *The Aeronautical journal*, 121:73–94, January 2017. <https://bit.ly/34TSkGz>.
- [2] T. Wilson, A. Castrichini, A. Azabal, J.E. Cooper, and M. Herring R. Ajaj. Aeroelastic behaviour of hinged wing tips. In *International Forum on Aeroelasticity and Structural Dynamics*, Como, Italy, June 2017. <https://www.researchgate.net/publication/318265002>.
- [3] A. Castrichini, T. Wilson, F. Saltari, F. Mastroddi, N. Viceconti, and J. E. Cooper. Aeroelastic flight dynamics coupling effects of the semi-aeroelastic hinge device. *Journal of Aircraft*, 57(2), March-April 2020. <https://doi.org/10.2514/1.C035602>.
- [4] A. Castrichini, V. Hodigere Siddaramaiah, D.E. Calderon, J.E. Cooper, T. Wilson, and Y. Lemmens. Nonlinear folding wing tips for gust loads alleviation. *Journal of Aircraft*, 53(5), September-October 2016. <https://arc.aiaa.org/doi/10.2514/1.C033474>.
- [5] A. Castrichini, T. Wilson, and J.E. Cooper. On the dynamic release of the semi aeroelastic wing-tip hinge device. In *6th Aircraft Structural Design Conference*, October 2018. <https://bit.ly/3cvGfKd>.
- [6] F. Fonte, Francesco Toffol, and Sergio Ricci. Design of a wing tip device for active maneuver and gust load alleviation. In *AIAA SciTech Forum*, Kissimmee, Florida, USA, January 2018. <https://arc.aiaa.org/doi/abs/10.2514/6.2018-1442>.
- [7] F. Toffol, F. Fonte, and S. Ricci. Design of an innovative wing tip device. In *International Forum on Aeroelasticity and Structural Dynamics*, Como, Italy, June 2017. <https://arc.aiaa.org/doi/abs/10.2514/6.2018-1442>.
- [8] Airbus. The albatross is inspiring tomorrow's aircraft wings. <https://bit.ly/2VI6ztM>.
- [9] Thomas Wilson, James Kirk, and John Hobday Andrea Castrichini. Small scale flying demonstrator of semi aeroelastic hinged wing tips. In *International Forum on Aeroelasticity and Structural Dynamics*, Savannah, Georgia, USA, June 2019. <https://bit.ly/2RRzRFv>.
- [10] Politecnico di Milano. Neocass. <https://www.neocass.org/?Home>.
- [11] A. Bérard, L. Cavagna, L. Riccobene A. Da Ronch and, and A.T. Isikveren S. Ricci and. Development and validation of a next-generation conceptual aero-structural sizing suite. In *26th INTERNATIONAL CONGRESS OF THE AERONAUTICAL SCIENCES*, 2008. https://www.researchgate.net/publication/248394518_Development_and_validation_of_a_next-generation_conceptual_aero-structural_sizing_suite.
- [12] L. Cavagna, S. Ricci, and L. Riccobene. A fast tool for structural sizing, aeroelastic analysis and optimization in aircraft conceptual design. In *50th AIAA/ASME/ASCE/AHS/ASC Structures, Structural Dynamics, and Materials Conference*, Palm Springs, California, USA, May 2009. <https://arc.aiaa.org/doi/10.2514/6.2009-2571>.
- [13] L. Cavagna, S. Ricci, and L. Travaglini. Aeroelastic analysis and optimization at conceptual design level using neocass suite. In *52nd AIAA/ASME/ASCE/AHS/ASC Structures, Structural Dynamics and Materials Conference*, Denver, Colorado, USA, April 2011. <https://arc.aiaa.org/doi/abs/10.2514/6.2011-2079>.
- [14] Airbus. *Airbus commercial aircraft AC A321*, 2005. <https://bit.ly/3eeGI4q>.
- [15] Airbus. *EASA type certificate data sheet for Airbus A318-A319-A320-A321*, 2013. <https://bit.ly/3gm5DF6>.
- [16] Airbus. *Airbus safety magazine*, 2006. <https://bit.ly/2zvthOU>.
- [17] Airbus a321. https://en.wikipedia.org/wiki/Airbus_A321.
- [18] MSC software. *Nastran quick reference guide*, 2012. https://simcompanion.mscsoftware.com/infocenter/index?page=content&id=DOC10004&actp=LIST_POPULAR.

APPENDIX

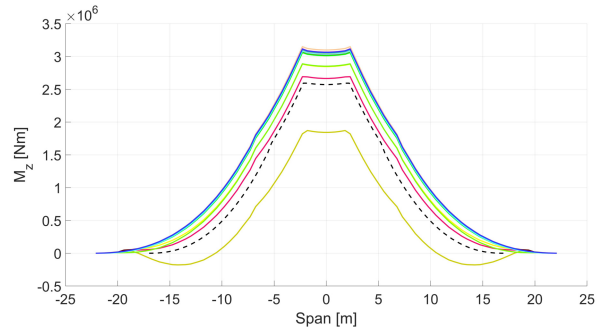
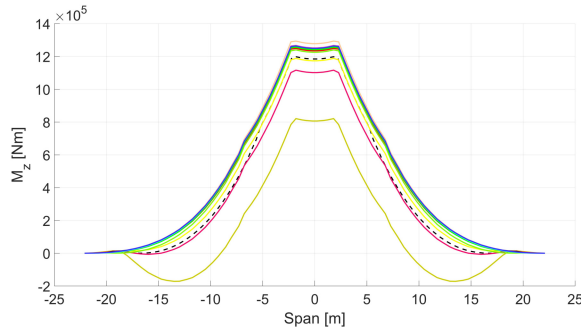


Fig. 18: Spanwise bending moment for each one of the 20 hinge configurations

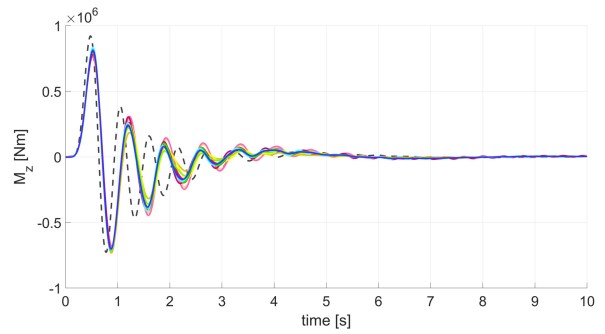
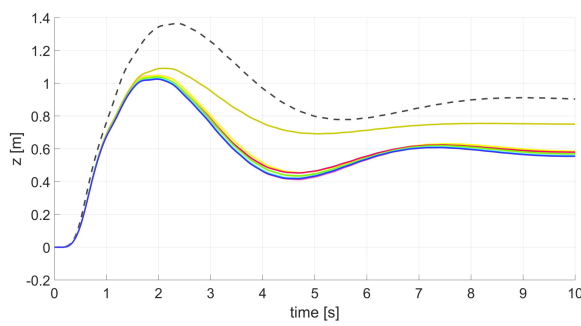


Fig. 19: Gust results for each one of the 20 hinge configurations

-- Baseline	— 84%, medium hinge stiffness
— 75%, Very low hinge stiffness	— 84%, high hinge stiffness
— 75%, low hinge stiffness	— 88%, Vlow hinge stiffness
— 75%, medium hinge stiffness	— 88%, low hinge stiffness
— 75%, high hinge stiffness	— 88%, medium hinge stiffness
— 81%, Vlow hinge stiffness	— 88%, high hinge stiffness
— 81%, low hinge stiffness	— 93%, Vlow hinge stiffness
— 81%, medium hinge stiffness	— 93%, low hinge stiffness
— 81%, high hinge stiffness	— 93%, medium hinge stiffness
— 84%, Vlow hinge stiffness	— 93%, high hinge stiffness
— 84%, low hinge stiffness	

Fig. 20: Legend for figures 18 and 19

For the sake of completeness, in this section all the results for each one of the 20 hinge combinations considered are reported. Figure (18) shows the spanwise bending moment both in cruise and pull-up manoeuvre, but it should be highlighted that the configuration with the hinge placed at 81% and a very low stiffness has been ignored in the previous results section because even though it contributes to load alleviation, its behaviour seems too weird and different with respect to all the others. As mentioned before, for gust analysis every hinge configuration proved to be beneficial for displacement and load alleviation, as showed in figure (19).